Physics of correlated double ionization of atoms in intense laser fields: Quasistatic tunneling limit

Gennady L. Yudin* and Misha Yu. Ivanov†
Femtosecond Science Program, Steacie Institute for Molecular Sciences, National Research Council of Canada, 100 Sussex Drive, Ottawa, Ontario, Canada K1A 0R6

(Received 7 September 2000; published 12 February 2001)

We revisit the recollision picture of correlated multiphoton double ionization of atoms in strong laser fields and develop consistent semiclassical model in the tunneling limit. We illustrate the model by applying it to helium and obtain quantitative agreement with recent experiments [B. Walker, E. Mevel, Baorui Yang, P. Breger, J. P. Chambaret, A. Antonetti, L. F. DiMauro, and P. Agostini, Phys. Rev. A **48**, R894 (1993); B. Walker, B. Sheehy, L. F. DiMauro, P. Agostini, K. J. Schafer, and K. C. Kulander, Phys. Rev. Lett. **73**, 1227 (1994)]. Developing the model, we address several problems of general interest, such as the reduction of intense field-assisted electron-ion collision to the field-free one and the total-cross-sections that include all inelastic channels. We describe a set of important physical effects responsible for the surprisingly high yield of doubly charged ions of noble gas atoms. All effects originate from the key role of the Coulomb potential and its interplay with the laser field. In addition to the Coulomb focusing of the oscillating trajectories onto the parent ion, other effects include transient trapping of electrons after tunneling in the vicinity of the parent ion, the creation of high-velocity electrons at all phases of the laser field, and the dominant role of collisional excitation of the parent ion followed by laser-assisted ionization.

DOI: 10.1103/PhysRevA.63.033404 PACS number(s): 32.80.Rm

I. INTRODUCTION

Correlated double ionization of atoms is one of the hottest topics in today's intense-field physics [2]. While correlated double ionization induced by one-photon absorption has been around for decades, atomic dynamics induced by the simultaneous absorption of tens of photons has been dominated by a single active electron [3]. It seemed very hard to make two electrons work together to absorb tens of photons, unless there was a few-photon resonance with a doubly excited state [4].

The deadlock was broken in 1992, with the experiments by Fittinghoff *et al.* [5] on double ionization of helium in intense near-infrared laser fields. The yield of singly charged helium was described extremely well by the single active electron approximation. However, double ionization signal exceeded the prediction based on the picture of sequential removal of two electrons by many orders of magnitude. This experiment, followed by the experiments [1,6,7], became a challenge for theoreticians. Exact *ab initio* calculations are exceedingly difficult even for the simplest two-electron atom, helium, due to very large changes of atomic energy on the subfemtosecond time scale [8].

Today we are witnessing a debate on the physical mechanisms underlying correlated double ionization in strong laser fields. The origin of this debate lies, perhaps, in the amazing simplicity of the physics responsible for almost all strong field effects, described by the so-called recollision picture [9,10].

In this picture, the active electron is promoted to the continuum by the laser field (e.g., via tunnel ionization), and, while oscillating in the laser field, returns and interacts with the parent ion. This model has been able to explain the generation of ultrahigh harmonics and above-threshold ionization in strong fields with remarkable clarity and almost no effort [11–13], but so far failed to quantitatively reproduce a very high yield of doubly charged ions [12] (with deviations up to two orders of magnitude). The key difficulty of the standard recollision theory [9,10,12] comes from the fact that when the electronic wave packet (or the corresponding ensemble of classical trajectories) is removed from the potential well via tunneling, it spreads very quickly in the directions perpendicular to the electric field. Consequently, there seems to be a very small chance of its recollision with the ionic core during oscillations in the field, although the core potential is able to modify this conclusion [14,15].

There has been very large progress in direct numerical solutions of time-dependent Schrödinger equation for strong-field double ionization [8], which (together with experiment) will provide the benchmark for the analysis. However, *ab initio* simulations are still limited to the wavelengths shorter than those used in experiments [1], stimulating the development of approximate models. These include numerical simulations for a model two-electron atom with each electron restricted to one dimension [16,17], strong-field *S*-matrix theory [18–20], a simplified two-electron model [21], and semiclassical approaches [12,14,15].

The latest experimental data measuring the ion recoil spectrum [22,23], experiments on the ellipticity dependence of double ionization [24], and the results of various approximate models [16–19,21,14,15] strongly support the recollision picture. Strong-field *S*-matrix theory of double ionization [18] so far provided the closest agreement with experiment (within a factor 2–3 for He). The main Feinmann diagram in this theory can be interpreted in terms of the recollision picture, although clear distinction between various contributions to this diagram is difficult. Such interpretation of *S*-matrix amplitudes in terms of classical trajecto-

*Email address: gennady.yudin@nrc.ca
†Email address: misha.ivanov@nrc.ca

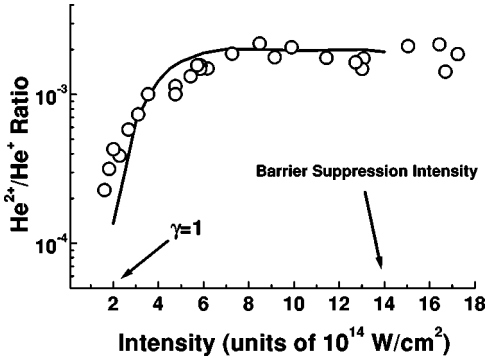

FIG. 1. Ratio of doubly to singly charged He as a function of laser intensity, for laser wavelength $\lambda = 780$ nm. Present calculation: solid curve. Experimental data Ref. [1]: open circles.

ries has been successfully done for single-electron processes [19,25] using saddle-point analysis of the multidimensional integrals. Similar analysis for two-electron processes for the main Feinmann diagram in the approach of Refs. [18,27] is mathematically very complex and so far has not been accomplished. However, such analysis has been performed for the simpler versions of two-electron strong-field *S*-matrix theory [26,27], which ignore ''soft'' rescattering of active electron off the ionic core prior to ''hard'' collision, which causes ionization of the parent ion.

The naive (standard) version of the recollision model misses several important physical effects, all resulting from the key role of the parent ion's Coulomb potential. The semiclassical calculation of Ref. [14] has stressed the important role of the so-called Coulomb focusing. An electron oscillating in the laser field and approaching the core with a large impact parameter is deflected by the Coulomb potential, leading to the possibility of efficient recollision with a much smaller impact parameter at later times. The Coulomb focusing, which arises from the interplay of the core potential and the laser field, significantly increases the probability of collision-assisted ionization [14].

The main problem of the model developed in Ref. [14] was the use of classical mechanics for describing the motion of both electrons following tunnel ionization of the active electron. This resulted in transitions of the second (bound in He^+) electron to unphysical states with energies significantly less than first excitation threshold $E_p \approx 40.8$ eV. These excitations where later converted into ionization by the laser field, providing large contribution to the probability of double ionization.

This paper has two goals. First, we develop consistent semiclassical theory of correlated double ionization in quasistatic tunneling limit, i.e., the Keldysh parameter $\gamma \ll 1$. Here $\gamma^2 = I_p/2U_p$, I_p is the ionization potential and $U_p = \mathcal{E}^2/4\omega_L^2$ is the average energy of electron oscillations in the laser field, atomic units are used throughout the paper. Our approach removes the problem of Ref. [14] by using correct quantum-mechanical cross sections for inelastic $e + He^+$ collisions and yields quantitative agreement with the experiment [1], see Fig. 1. Some aspects of our model are similar to those of Ref. [15], however, we (i) do not assume separability of the electronic motion along and perpendicular to the laser field, (ii) fully include collisional excitation, relating intense-field collisions to the field-free ones, and (iii) for the active electron, we use adequate for tunneling set of initial conditions both perpendicular and along the electric field.

Second, we describe several physical effects that play an important role in the problem of correlated double ionization in strong laser fields. In addition to the Coulomb focusing described previously [14], these include (i) reduced spreading of the electron trajectories in the continuum during the first laser cycle after its birth, also found in Ref. [15], (ii) transient trapping of electrons in Rydberg orbits after tunneling, (iii) energy gain in soft collisions with the core, which allows the electron to reach the largest possible return energy $\sim 3U_p$, irrespective of the instant of tunneling, and (iv) the dominant role of collisional excitation of He^+ followed by ionization in the laser field.

Developing a complete a semiclassical model, we had to address two problems of general interest. These are (1) relationship between the total cross sections of intense field-assisted inelastic electron-ion collisions and the field-free problem, and (2) total cross sections of all collisional excitation and ionization channels for energies from first excitation threshold up to energies $E \gg I_p$.

We illustrate the physics of correlated multiple ionization in intense fields, general to all high ionization potential atoms or ions, using the example of helium. Double ionization of helium has an important peculiarity: two electrons involved in the process start in the singlet ground state, and the singlet character of their coupling is preserved during ionization. This is absent in other noble gases. For example, in Ne active electron is in singlet coupling with only one of seven electrons left in the outer shell, suppressing the polarization effects. In our calculations we use polarization-averaged cross sections for both collisional ionization and excitation, as would be generally correct for all other noble gas atoms.

For helium, polarization-averaged cross sections underestimate direct collisional ionization by about a factor of 2 [15]. However, we show that total yield of doubly charged ions is dominated by collisional excitation of the parent ion, followed by laser-induced ionization (factor of 3 at $I \sim 10^{15}$ W/cm^2 and factor of 40 at $I \approx 3 \times 10^{14}$ W/cm^2). For excitation, the spin-polarization effects are expected to be much weaker and have different energy dependence (note, that in elastic $e + He^+$ collisions the triplet cross section is larger than singlet).

In the absence of reliable data on spin assymmetry in collisional excitation, we decided to use polarization-averaged cross sections. In the next publication, we will present a detailed discussion of the polarization effects in helium for total inelastic cross sections, as well as the extension of our model to the case of inermediate values of the Keldysh parameter $\gamma \sim 1$, where deviations from the quasistatic tunneling regime become significant.

II. THE MODEL

A. Basic assumptions

In the spirit of recollision picture, we break the process of double ionization into four steps: (1) tunneling of the first

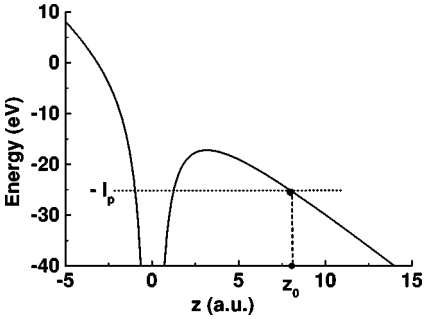

FIG. 2. Pictorial scheme of tunnel ionization, z_0 is the ''exit'' point.

(active) electron out of atomic potential well, (2) its motion in the laser field and the potential of the parent ion, (3) recollision with the parent ion leading to either ionization or excitation of the parent ion, and (4) further evolution of the excited ion in the laser field. At every step we include both the laser field and the Coulomb interactions on equal footing and with adequate accuracy.

Tunnel ionization of the active electron is described using adiabatic approximation of Dykhne [28]. At each phase $\phi=\omega_L t$ of the laser field $\mathcal{E}\cos\omega_L t$ a swarm of trajectories is started on the other side of the barrier created by the binding potential and the laser field, see Fig. 2. The number of trajectories $N(\phi)$ is proportional to the quasistatic tunneling probability at phase ϕ, $N(\phi)\propto\exp[-2(2I_p)^{3/2}/3\mathcal{E}\cos\phi]$.

Electron motion in the continuum is described classically including both the laser field and the Coulomb potential of the core. The ensemble of initial conditions is chosen to mimic the wave packet as it emerges from under the instantaneous barrier, see Fig. 2. The distribution of coordinates and velocities parallel and perpendicular to the laser polarization is taken to correspond to tunnel ionization [29–31] and is discussed in detail in the following subsection. As the swarm of trajectories is propagated in the laser field and the potential of the parent ion, its spreading simulates spreading of the wave packet.

Each trajectory $\mathbf{R}(t)$ is monitored for all approaches to the parent ion, i.e., we record all local minima in time-dependent distance $|\mathbf{R}(t)|=R(t)$ and the corresponding velocities $\mathbf{v}(t)$. While there could be many approaches (many returns), we almost never observe more than one ''hard'' collision capable of knocking the second electron out. Still, many ''soft'' collisions are very important as they determine the impact parameter and the impact velocity during the hard collision.

Inelastic $e+\mathrm{He}^+$ collisions are described using quantum-mechanical cross sections, with the laser field accounted for within the theory of semisudden perturbation. As shown below, the contribution of the laser field to the classical action (or to the semiclassical phase of the wavefunction) during the nonadiabatic stage of collision τ is small compared to unity. This allows us to use *field-free* cross sections of all inelastic collisional channels as long as we properly take into account the action of the laser field before and after the collision.

B. Quasistatic tunnel ionization and initial conditions for classical trajectories

Following Refs. [29–31], in the limit of small Keldysh parameter $\gamma\ll 1$, the instantaneous tunneling rate at the phase $\phi=\omega_L t$ is

$$\Gamma_{qs}(\phi)=A_{n^*lm}(\mathcal{E}\cos\phi)^{1+|m|-2n^*}\exp\left(-\frac{2(2I_p)^{3/2}}{3\mathcal{E}\cos\phi}\right). \tag{1}$$

Here A_{nlm} is a factor depending on the effective principal quantum number $n^*=Z/\sqrt{2I_p}$ (Z is the ion charge), angular momentum l, and its projection on the laser polarization m [31]. We use this formula to weight the contribution of trajectories started at every phase ϕ.

We now have to specify the ensemble of initial conditions for the trajectories started at every phase ϕ, i.e., the distributions z,v_z along the direction z of the electric field and r,v_r in the perpendicular plane (r is the cylindrical coordinate).

Since the electric field does not act in the lateral direction, the lateral distribution of electrons emerging from under the barrier is the same as the well-known distribution at infinity, in the tunneling limit [31]:

$$w(v_r)=w(0)\exp\left(-\frac{\sqrt{2I_p}v_r^2}{\mathcal{E}\cos\phi}\right). \tag{2}$$

In fact, this distribution ignores rescattering of the electrons on the parent ion. Therefore, it is ideally suited for our purposes—distribution immediately after tunneling. The radial distribution $w(r)$ is given by the square of the Fourier transform of $\sqrt{w(v_r)}$.

The longitudinal distribution $w(v_z)$ given in Ref. [31] refers to the final energies of the electron long after tunneling. This energy distribution is completely dominated by acceleration in the electric field and is determined only by the phase of birth ϕ. The situation is also not simpler at short times near the instant of tunneling due to large contribution of virtual transitions to the adiabatic Dykhne amplitude. The initial conditions for the classical trajectories cannot include the contribution of virtual transitions that decay back to the ground state. We resolve the problem by using exact solutions for tunneling in a static electric field. In this limit the wave function of the electron after tunneling is proportional to the Airy function $\Psi(z)\sim\mathrm{Ai}[(2\mathcal{E})^{1/3}(z-z_0)]$, where z_0 is the outer classical turning point, see Fig. 2. While oscillations of the Airy function at $z>z_0$ reflect acceleration of the outgoing electron by the laser field, its decay under the barrier reflects the uncertainty in the position of the electron at the moment of tunneling. The characteristic width of this distribution is $\Delta z\approx(2\mathcal{E})^{-1/3}$, and the corresponding width of the velocity distribution is $\Delta v_z\approx(2\mathcal{E})^{1/3}$. Since the Gaussian form is general for adiabatic bound-free transitions (see, e.g., Ref. [32]) we use Gaussian form for both $w(z)$ and $w(v_z)$ centered around $z=z_0$ and $v_z=0$ (see Fig. 2) and substitute $\mathcal{E}\to\mathcal{E}\cos\phi$ for every phase of birth.

Given the initial conditions, the trajectories of active electron are found using the Newton equation

$$\ddot{\mathbf{R}} = -\mathbf{R}/R^3 - \vec{\mathcal{E}}\cos\omega_L t. \tag{3}$$

C. Three stages of recollision

All collisions between the active electron and the parent ion can be divided into adiabatic (''soft'') and nonadiabatic (''hard'') collisions. Only hard collisions cause excitation and/or ionization of ground-state He^+. Nevertheless, soft collisions play a crucial role in determining the energy of the returning electron during the hard collision.

The transition between the regions of adiabatic and nonadiabatic evolution during the hard collision is characterized by the ''adiabatic radius''

$$\rho_a = v/\Omega, \tag{4}$$

where Ω is the characteristic transition frequency and v is the characteristic velocity during the collision (without the contribution of the Coulomb potential). Taking v and Ω to correspond to the maximum in the total cross section of all excitation and ionization channels for $e+He^+$ (see below), we find $\rho_a \sim 1$. The characteristic duration of nonadiabatic interaction $\tau \sim 1/\Omega$ is also on the order of one atomic unit.

Hence, the recollision dynamics can be divided into three distinct stages. The first stage, which starts after tunnel ionization of active electron, is adiabatic with respect to collisional excitation and/or ionization of inner (passive) electron. During this stage, the active electron experiences long-range soft collisions with the parent ion, which may significantly modify its trajectory and change its energy (due to the presence of the laser field), but do not lead to additional excitation and/or ionization.

The second stage is that of hard collision (if such collision ever occurs). The overall dynamics is nonadiabatic ($\Omega\tau_a \sim 1$), but for the laser field the excitation and/or ionization of the parent ion is sudden:

$$V_L\tau \sim \mathcal{E}\rho_a\frac{1}{\Omega} = \frac{\mathcal{E}v}{\Omega^2} \ll 1. \tag{5}$$

In our case of $e+He^+$ collisions the coefficient v/Ω^2 is very close to unity for v and Ω corresponding to the maximum of the total inelastic cross section. This simplifies criterion Eq. (5) to

$$\mathcal{E} \ll 1. \tag{6}$$

The inequality [Eq. (5)] allows us to use the theory of semisudden perturbations (see Appendix A). In its lowest order, the problem is rigorously reduced to the *laser field-free* excitation during the time τ of hard collision, allowing us to use cross sections of field-free collisions.

The third stage begins when the active electron leaves the region of nonadiabatic interaction. Once again, the laser field plays a crucial role at this stage. Since we are only interested in the total yield of He^{2+} and not in the energy and angular distributions of the electrons, it is sufficient to evaluate the probability of laser-induced ionization of the excited states created during the second stage. If He^+ is left in the ground state, its ionization is negligible in the intensity region of interest ($I \leqslant 2\times 10^{15}$ W/cm^2). On the other hand, every excited state will be ionized by the laser field with unit probability (already beginning with $I \approx 3.4\times 10^{13}$ W/cm^2 the potential barrier for ionization is suppressed below the first excited state of He^+).

From the mathematical perspective, these three stages correspond to breaking the time-evolution operator into three parts and making different approximations for each. In our model, for each classical trajectory of the active electron, the time evolution of the passive electron is given by

$$|\Psi(t)\rangle = \hat{S}(t,t_c+\tau/2)\hat{S}(t_c+\tau/2,t_c-\tau/2) \times \hat{S}(t_c-\tau/2,t_0)|\Psi(t_0)\rangle, \tag{7}$$

where t_0 is the moment of tunneling of the active electron, t_c is the moment of hard collision, and τ is the duration of hard collision. Time evolution of the passive electron is determined by the Hamiltonian

$$\hat{H}(t) = \hat{H}_i + V_L + V_{ee}, \tag{8}$$

where $\hat{H}_i$ is the Hamiltonian of He^+ ion, V_L is the interaction of the passive electron with the laser field, and V_{ee} is the electron-electron interaction.

At the first stage of recollision, which starts immediately after tunneling, the laser field is too weak and the electron-electron interaction is too adiabatic to induce any transitions. Therefore, before hard collision, $t < t_c - \tau/2$, we neglect V_L and V_{ee} for the passive electron. The time-evolution operator $\hat{S}(t_c-\tau/2,t_0)$ is determined by the Hamiltonian

$$\hat{H}(t_0 \leqslant t < t_c - \tau/2) \approx \hat{H}_i \tag{9}$$

and the passive electron remains in the ground state of He^+.

At the second stage $V_L\tau \ll 1$ [see Eq. (5)], so that the effect of the laser field is small and time-evolution operator $\hat{S}(t_c+\tau/2,t_c-\tau/2)$ is determined by the Hamiltonian

$$\hat{H}(t_c-\tau/2 \leqslant t \leqslant t_c+\tau/2) \approx \hat{H}_i + V_{ee}. \tag{10}$$

Hence, the evolution during the collision is the same as for the field-free case. Note, however, that the collision energy was supplied by the laser field.

We now insert the complete basis set of field-free states of He^+ at the end of the second stage:

$$|\Psi(t_c+\tau/2)\rangle = \sum_n |n\rangle\langle n|\exp\left[-i\int_{t_c-\tau/2}^{t_c+\tau/2} dt'(\hat{H}_i+V_{ee})\right] \times |\Psi(t_c-\tau/2)\rangle = \sum_n a_n|n\rangle. \tag{11}$$

Here a_n are the amplitudes of the field-free excitation and/or ionization of He^+ ground state created at the beginning of

the third stage. We stress that the energy of the active electron, which determines the amplitudes a_n, is acquired from the laser field during the first stage of recollision.

At the third stage the time evolution is determined by the complete Hamiltonian $\hat{H}$ [see Eq. (8)]. While all states $|n\rangle$ evolve in the laser field, the normalization requires that

$$\sum_n |a_n(t\to+\infty)|^2 = \sum_n |a_n(t_c+\tau/2)|^2, \tag{12}$$

where $|a_n(t\to+\infty)|^2$ are populations of the field-free excited states of He^+ after the end of the pulse. We assume that every excited bound state of He^+ ionizes while what is left in the ground state after $t_c+\tau/2$ remains intact. This is justified as long as the probablitity of direct tunnel ionization from He^+ ground state is negligible. Hence, the above equation reduces to

$$\sum_{n_{\rm cont}} |a_n(t\to+\infty)|^2 = \sum_{n\neq 0} |a_n(t_c+\tau/2)|^2, \tag{13}$$

where $|n_{\rm cont}\rangle$ are the field-free continuum states of He^+. Thus, the total probability of excitation and ionization at $t=t_c+\tau/2$ is transferred into the total ionization probability at the end of the third stage.

In the quantum evolution there has to be a sum over all moments of collision t_c and moments of tunneling t_0. In our approach this is accounted for by averaging over the ensemble of classical trajectories characterized by distributions of t_0 and t_c.

Taking into account the laser field only at the first and third stages of recollision is based on the inequality $V_L\tau \ll 1$. This requirement is not met in the case of excitiation of long-lived autoionizing resonances, which yield doubly rather than singly charged ions due to the presence of a strong laser field. Also, at low intensities, where the collision energy is too low and all field-free excitation channels are closed, the lowest-order term in the expansion in powers of $V_L\tau$ is equal to zero, so that higher-order terms dominate. This limits the applicability of our approach at low intensities.

D. Inelastic cross sections

As shown above, due to short time of nonadiabatic collision, we can reduce the problem to using cross sections of *field-free* excitation and ionization in all channels, followed by the evolution of the excited states in the laser field.

The region of active electron energies that is of interest in the recollision problem at intensities $I\leqslant 2\times10^{15}$ W/cm^2 and laser wavelength in the near infrared is between the excitation thereshold $E_p\approx 40.8$ eV and up to $E\approx 3.2U_p$ ($U_p\approx 120$ eV at $I=2\times10^{15}$ W/cm^2 and $\lambda\approx 800$ nm). In principle, the general theory of collisional excitation in this broad energy range is quite complicated, especially near the thresholds for each channel. However, since we are interested in the total yield and integrate over all energies of incident electron, we do not have to include fine structures and oscillations of cross sections for each individual channel within narrow energy intervals. We only need to use total cross sections averaged over the fine structure.

1. Ionization

Cross sections of direct collisional ionization of He^+ are well-known from experiments [33] and can be fitted by empirical and semiempirical formulas reviewed in Ref. [34]. We use the formula based on correct limits at high and near-threshold energies:

$$\sigma_{ion}(E)\approx \pi a_0^2\left(\frac{2\ {\rm Ry}}{I_p}\right)^2 F(E/I_p),$$

$$F(x)=\frac{1}{x}\left[A\ln x + B\left(1-\frac{1}{x}\right)-\frac{C}{x}\ln x\right], \tag{14}$$

where a_0 is the Bohr radius, $I_p\approx 54.4$ eV is the ionization potential of He^+, and the coefficients are $A=0.285$, $B=1.28$, and $C=1.36$. The first term describes the well-known high-energy limit, and the constant A is determined from the Bethe-Born approximation for the Hydrogen atom [35]. The second term is used to fit the near-threshold behavior, while the third term is used to fit the intermediate energy region.

Reasonable agreement with experimental data can also be obtained using the generalization of the original 1912 Thomson approach [36], developed by Gryzinski [37] in 1965:

$$\sigma_{ion}^{(Gr)}(E,I_p)=\pi a_0^2\left(\frac{2{\rm Ry}}{I_p}\right)^2 {\rm Gr}(E/I_p)$$

$${\rm Gr}(x)=\frac{1}{x}\left(\frac{x-1}{x+1}\right)^{3/2}\left[1+\frac{2}{3}\left(1-\frac{1}{2x}\right)\ln(e+\sqrt{x-1})\right]. \tag{15}$$

This formula is very attractive for our purposes since its physical origin—energy and momentum conservation laws—is equally applicable to collisional excitation, which is much less studied. In fact, there are virtualy no experimental and theoretical data on total excitation cross sections in a broad energy range. Below we use the analog of Eq. (15) to fit available data on excitation cross sections.

Well-known defects of the Gryzinski formula are the shift of maximum in ionization cross section to higher energy (for He^+ it is shifted from $E_m=179.9$ eV to $E_m^{(Gr)}=205.6$ eV) and the wrong shape of the curve at intermediate energies. They are easily corrected by treating Eq. (15) as a semi-empirical formula, with I_p as a fitting parameter:

$$\sigma_{ion}^*(E)=\alpha_{ion}\sigma_{ion}^{(Gr)}(E,I_p^*),\quad I_p^*=\beta_{ion}I_p. \tag{16}$$

For $\alpha_{ion}=0.815$ and $\beta_{ion}=0.89$ Eq. (16) fits both experimental data and Eq. (14) quite well, except for a very narrow region near the threshold. As shown below, the same set of parameters α_{ion},β_{ion} allows us to obtain good fit to the excitation cross sections.

2. Excitation

Collisional excitation followed by laser-induced ionization dominates total inelastic cross section. Unfortunately, there are only few relevant experiments that give data on $|1S\rangle \rightarrow |2S\rangle$ [38] and $|1S\rangle \rightarrow |2P\rangle$ [39] transitions (in the latter case, only relative cross sections were measured, and then they were normalized to the theoretical Coulomb-Born results at $E=217$ eV).

There are many theoretical papers that go beyond Born and Coulomb-Born approximations, including the so-called eikonal approaches, which allow one to obtain relatively reliable data in a broad energy range. Using experimental data for $|1S\rangle \rightarrow |2S\rangle$ transition as a benchmark, we conclude that the conventional Coulomb-Born cross sections lie above the observation curve everywhere, while the plane-wave Glauber approach improves the agreement but goes smoothly to zero at the threshold (instead of a nonzero value). Coulomb-eikonal results (see, e.g., Refs. [40,41]) provide clear improvement near the threshold (due to inclusion of the Coulomb potential), exhibit better behavior at intermediate energy range, and approach the Coulomb-Born results at high energies. Furthermore, for $|1S\rangle \rightarrow |2P\rangle$ transition the Coulomb-eikonal method yields reasonable results that generally lie between the plane-wave Glauber and unitarized Coulomb-Born curves.

Reference [40] gives cross sections of $|1S\rangle \rightarrow |nS,nP\rangle$ transitions for hydrogenlike ions with n ranging from two to infinity. We use the properties of n scaling found in this paper to find integral cross sections for all $|n,l\rangle$. However, near the excitation threshold the results of the approach in Ref. [40] do not reproduce experimental data. We correct this behavior based on the results of eikonal partial wave theory (also called Coulomb-projected eikonal model) [41], which gives better agreement with experiment in this region, but was only applied to $|1S\rangle \rightarrow |2S,2P\rangle$ channels.

Our procedure for finding total cross sections of all exciation channels in He is as follows: First, we use experimental data of Refs. [38,39] to obtain total $|1S\rangle \rightarrow |n=2\rangle$ cross section and compare with total $|1S\rangle \rightarrow |n=2\rangle$ cross section obtained from Refs. [40,41]. We fit the experimental data with a smooth curve taking into account the correct threshold behavior, i.e., energy independence near the threshold for collisions with positive ions.

Then, using scaling from the theoretical data [40] and taking into account correct threshold behavior, we obtain $|1S\rangle \rightarrow |nS+nP\rangle$ cross sections. As expected, the $|1S\rangle \rightarrow |nP\rangle$ transition gives the main contribution to the total $|1S\rangle \rightarrow |n\rangle$ cross section (integrated over all angular momenta). We now check that the n dependence of $|1S\rangle \rightarrow |nS+nP\rangle$ cross sections is close to the one that we have derived for total $|1S\rangle \rightarrow |n \leqslant 4\rangle$ cross sections, using the recommendations of Ref. [42]. We then use this n dependence to correct the $|1S\rangle \rightarrow |nS+nP\rangle$ cross sections from Ref. [40] by including omitted $|1S\rangle \rightarrow |3D,4D,4F\rangle$ transitions. For $n \geqslant 5$ the approximate relationship $\sigma_{\rm exc}(E_{n+1}) - \sigma_{\rm exc}(E_n) \propto n^{-3}$ is valid.

Figures 3 and 4 summarize our results for total excitation and excitation plus ionization cross sections between the first excitation threshold E_p and 800 eV.

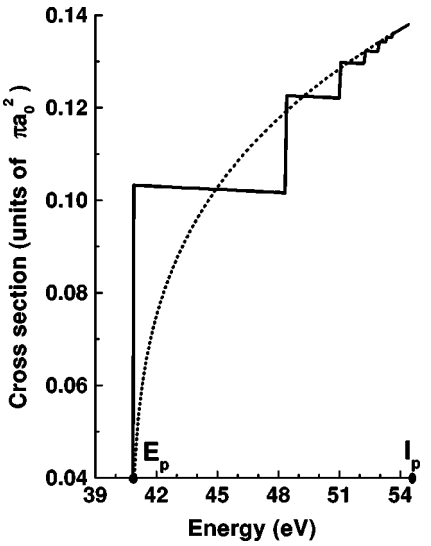

FIG. 3. Total cross section of He^+ excitation by electron impact at energies between first excitation threshold E_p and ionization threshold I_p: solid curve. Approximation [Eq. (17)]: dotted curve.

At $E \geqslant 100$ eV the total cross section can be fitted by

$$\sigma_{inel}(E) \approx \pi a_0^2 \left(\frac{4\mathrm{Ry}^2}{EI_p} \right) F_{inel}(E/E_p),$$

$$F_{inel}(x) = \ln x + 1.47\left(1 - \frac{1}{x}\right) - 1.62\frac{\ln x}{x}. \qquad (17)$$

Above ionization threshold, we found a remarkable semiempirical scaling relationship between the total excitation cross section, its value at the ionization threshold $\sigma_{\rm exc}(I_p)$, and the energy $E_m \approx 179.9$ eV at which the ionization cross section $\sigma_{ion}(E)$ reaches its maximum value:

$$\sigma_{\rm exc}(E \geqslant I_p) \approx \frac{\sigma_{\rm exc}(I_p)}{1 + 0.55G(E)},$$

$$G(E) = \frac{E - I_p}{E_m}, \qquad (18)$$

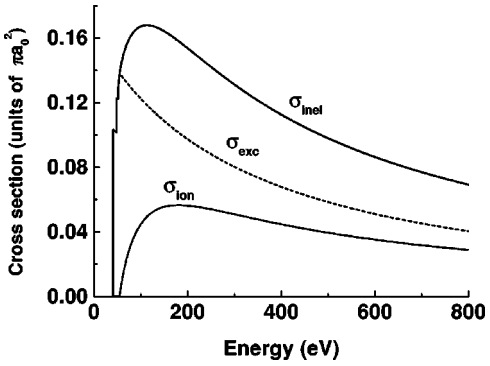

FIG. 4. Cross sections of inelastic $e + He^+$ collisions: ionization σ_{ion}, excitation $\sigma_{\rm exc}$, and total σ_{inel}.

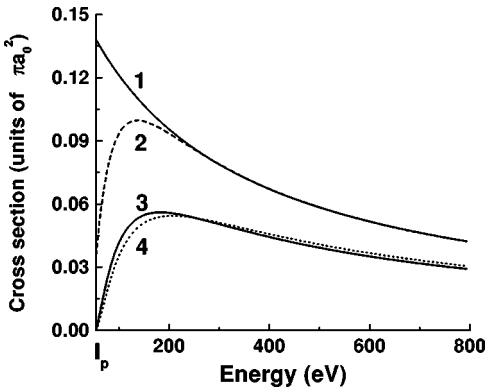

FIG. 5. Correlation between total excitation and total ionization cross sections of $e+\mathrm{He}^+$ collision at energies above I_p. Scaling law [Eq. (18)] for total excitation cross section: solid curve 1. Total excitation cross section calculated using Eq. (20): dashed curve 2. Experimental data for total ionization cross section fitted with Eq. (14): solid curve 3. Gryzinski formula [Eq. (15)] for total ionization cross section: dotted curve 4. Renormalized Gryzinski formula [Eq. (16)] is virtually indistinguishable from curve 3. Generalization of this renormalized formula for total excitation cross section [see Eq. (19)] is virtually indistinguishable from curve 2.

where $\sigma_{\mathrm{exc}}(I_p)\approx 0.138\pi a_0^2$. Physically, the scaling parameter $G(E)$ relies on the natural energy scale E_m at energies above I_p.

Our scaling relationship is related to energy and momentum conservation during collision, since it can be obtained from simple generalization of the Thomson and Gryzinski approaches (which are based on these conservation laws) to the case of total excitation cross sections. Such generalization corresponds to substituting I_p with the first excitation threshold E_p in Eq. (15), retaining the same corrections as for ionization cross section, Eq. (16):

$$\sigma^*_{\mathrm{exc}}(E)=\alpha_{\mathrm{exc}}\sigma^{(Gr)}_{\mathrm{exc}}(E,E^*_p) = \alpha_{\mathrm{exc}}\pi a_0^2\left(\frac{2\mathrm{Ry}}{E^*_p}\right)^2 \mathrm{Gr}(E/E^*_p), \quad E^*_p=\beta_{\mathrm{exc}}E_p \tag{19}$$

with the parameters α_{exc} and β_{exc} the same as for ionization, $\alpha_{\mathrm{exc}}=0.815$, $\beta_{\mathrm{exc}}=0.89$. This formula reproduces our data and the scaling relationship Eq. (18) at intermediate and high energies.

The same result is obtained using similar generalization of the equation (14), with a substitution of I_p with E_p (without any renormalizations):

$$\sigma_{\mathrm{exc}}(E)\approx \pi a_0^2\left(\frac{2\mathrm{Ry}}{E_p}\right)^2 F(E/E_p). \tag{20}$$

This expression fits our data at energies above $E\approx 4I_p$ (see Fig. 4). All correlations between total excitation and total ionization cross sections are shown in Fig. 5.

To summarize, we can now give a simple semiempirical prescription for obtaining the excitation cross sections from experimental data on ionization cross sections at $E\geqslant I_p$. First, one has to fit experimental data on ionization cross sections to obtain $F(E/I_p)$. Second, replacing I_p with E_p yields reliable fit to excitation cross sections above $E\approx 4I_p$. This allows one to obtain $\sigma_{\mathrm{exc}}(I_p)$ in the scaling relationship Eq. (18) and hence find $\sigma_{\mathrm{exc}}(E\geqslant I_p)$.

Finally, below ionization threshold, the excitation cross sections are approximately constant within the intervals $E_n \leqslant E<E_{n+1}$ where $E_n=Z^2/2-Z^2/(2n^2)$ is the excitation energy of nth shell of He^+. The values $\sigma_{\mathrm{exc}}(E_n)$ for $n=2,3,4$ are approximately equal to 0.102, 0.123, and 0.130 (in units of πa_0^2).

The range of energies between E_p and I_p is rather narrow compared to the typical width of electron energy distribution in our case, $3.2U_p$. We can replace the stepwise behavior of $\sigma_{\mathrm{exc}}(E\leqslant I_p)$ in this region with a smooth curve

$$\sigma_{\mathrm{exc}}(E\leqslant I_p)\approx\sigma_{\mathrm{exc}}(I_p)[\zeta(E)]^{1/4}, \quad \zeta(E)=\frac{E-E_p}{I_p-E_p}, \tag{21}$$

where $\sigma_{\mathrm{exc}}(I_p)\approx 0.138\pi a_0^2$.

E. Probabilities

In the semiclassical approach, it is not sufficient to know integral cross sections of collision. For each trajectory of the active electron, we have to introduce the corresponding probability of collisional excitation and/or ionization $w(E,\rho)$, which depends on energy and impact parameter. We find $w(E,\rho)$ from the asymptotic behavior of probability for large impact parameters ρ and using the normalization condition

$$\sigma(E)=2\pi\int_0^\infty d\rho\,\rho w(E,\rho). \tag{22}$$

Note that we are using *field-free* cross sections from the standard collision theory. These cross sections refer to the energy of the electron at infinity. Therefore, from the velocity v_c and the minimal distance from the core ρ_c at the moment of collision t_c we have to find the values at infinity v_∞,ρ_∞ corresponding to v_c,ρ_c in the *field-free* collision. These values are found from energy and momentum conservation laws:

$$v_\infty^2=v_c^2-\frac{2}{\rho_c}, \tag{23}$$

$$\rho_\infty=\left(\frac{v_c}{v_\infty}\right)\rho_c. \tag{24}$$

To illustrate our approach, let us start with an example of a specific excitation channel, $|i\rangle\rightarrow|f\rangle$ with a cross section $\sigma_{fi}(E)$ and a transition frequency Ω_{fi}. The asymptotic behavior of $w_{fi}(E,\rho)$ for large impact parameters ρ depends only on the ratio ρ/ρ_a, where $\rho_a=v/\Omega_{fi}$ is the adiabatic radius [see Eq. (4)] for the transition $|i\rangle\rightarrow|f\rangle$:

$$w_{fi}(E,\rho)\propto g(\rho/\rho_a)\equiv\mathcal{K}_0^2(\rho/\rho_a)+\mathcal{K}_1^2(\rho/\rho_a). \tag{25}$$

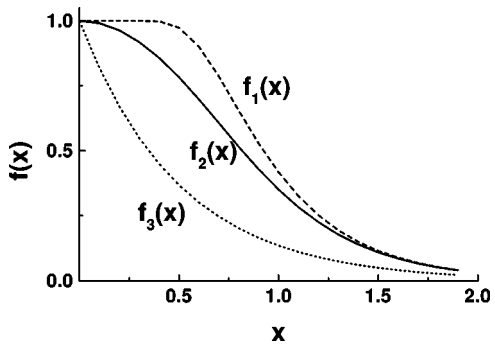

FIG. 6. Different models $f_m(x)$ [see Eq. (28)] for the dependence of inelastic collision probability [Eq. (25)] on the scaled impact parameter ρ/ρ_a, where ρ_a is the adiabatic radius, Eq. (4).

Here $\mathcal{K}_n(z)$ are the modified Bessel functions [43]. This expression is standard for the semiclassical theory of Coulomb excitation (see, e.g., Ref. [44]).

Since at small ρ/ρ_a the probability $w_{fi}(E,\rho)$ is weakly dependent on ρ/ρ_a, we assume that $w_{fi}(E,\rho)$ depends only on ρ/ρ_a for all impact parameters:

$$w_{fi}(E,\rho) \propto f(\rho/\rho_a), \tag{26}$$

where $\rho_a = v/\Omega_{fi}$, and the specific forms of $f(\rho/\rho_a)$ are given below. Even if this assumption is crude for a specific transition, it is sufficient for our purposes since we are only interested in total probability summed over all inelastic channels. This assumption, together with Eq. (22) gives one-to-one correspondence between $w_{fi}(E,\rho)$ and $\sigma_{fi}(E)$:

$$w_{fi}(E,\rho) = \left(\frac{\sigma_{fi}(E)}{2\pi\mathcal{J}}\right)\left(\frac{\Omega_{fi}}{v}\right)^2 f(\rho/\rho_a). \tag{27}$$

Here

$$\mathcal{J} = \int_0^\infty dx\, x f(x). \tag{28}$$

The function $f(x)$ has to satisfy the asymptotic behavior in Eq. (25), $f(x) \to g(x)$ at $\rho \gg \rho_a$. We use three different models for $f(x)$:

$$f_1(x) = 1 - \exp[-g(x)],$$

$$f_2(x) = \frac{g(x)}{1+g(x)},$$

$$f_3(x) = \exp(-2x), \tag{29}$$

where the last function uses only asymptotic behavior of $g(x)$ at $x \to \infty$. The functions $f_m(x)$ are shown in Fig. 6. While we prefer $f_1(x)$ and $f_2(x)$ for their more physically correct behavior at small x, we find that results for the total yield of He^{2+} are essentially independent of the choice of $f_m(x)$. This reflects the fact that trajectories of the active electron after tunneling almost homogeneously fill the region of essential impact parameters $\rho \sim \rho_a$.

For completness, we also use the standard model of a nearly hard sphere:

$$w_{fi}^{(0)}(\rho,E) = \exp(-\rho^2/\rho_0^2), \tag{30}$$

where ρ_0 is determined by the cross section of the $|i\rangle \to |f\rangle$ transition:

$$\sigma_{fi}(E) = \pi\rho_0^2. \tag{31}$$

We stress that ρ_0 has no relationship to the adiabatic radius and is typically much smaller than ρ_a. The results obtained using the hard-sphere model are generally higher than those obtained using correct long-range behavior. This reflects inhomogeneous distribution of impact parameters on the scale of $\rho_0 \ll \rho_a$, with extra density of trajectories within $\rho \leqslant \rho_0$.

Now, we have to use these results to obtain the expression for the total probability $w(E,\rho)$ integrated over all open inelastic channels. In principle, one could apply the above procedure to all excitation and ionization channels, integrating over all final bound and free states. However, this requires the knowledge of differential ionization cross sections $d\sigma_{ion}/dE_f$ [E_f is the final energy of ejected (passive) electron], which are not known for $E \sim I_p$ with sufficient accuracy.

Fortunately, for high energies of the incoming active electron, $E \gg I_p$, there is one-to-one correspondence between total inelastic cross section $\sigma(E)$ integrated over all open excitation and ionization channels and the semiclassical total transition probability $w(E,\rho)$ [45]. As shown in Ref. [45], when calculating $w(E \gg I_p,\rho)$ one can introduce the mean transition frequency $\bar{\Omega}(E,\rho)$. For hydrogenlike ions $\bar{\Omega}(E,\rho) = q(\rho)Z^2$, where the factor $q(\rho)$ is in the interval 0.4–0.5. Since the dependence of $w(E,\rho)$ on ρ is weak for $\rho < \rho_a$, one can also introduce the mean transition frequency for the cross sections $\bar{\Omega}(E \gg I_p) = \bar{q}Z^2$, where $\bar{q}$ was found to be $\bar{q} = 0.465$ [45]. For He^+ this gives $\bar{\Omega}(E \gg I_p) = \bar{\Omega}_\infty = 1.86$ a.u.

On the other hand, the mean transition frequency can also be introduced at energies $E \leqslant I_p$. Cross sections for each excitation channel remain approximately constant within the narrow energy interval above its appearance threshold and below I_p. Therefore, we define $\bar{\Omega}(E \leqslant I_p)$ as

$$\bar{\Omega}(E) = \frac{\sum_f \Omega_{fi}\sigma_{fi}(E)}{\sum_f \sigma_{fi}(E)} \tag{32}$$

with $|i\rangle$ the ground state of He^+. The sums are taken over all open channels $|f\rangle$.

For energies just above first excitation threshold in He^+ the transition frequency is that of the $|1S\rangle \to |n=2\rangle$ transition, $\bar{\Omega}_0 = \Omega_{21} = 1.5$ a.u. At $E = I_p$ the mean transition frequency is $\bar{\Omega}_I \approx 1.58$ a.u. Mean frequency between E_p and I_p is shown in Fig. 7. Since this energy interval is relatively

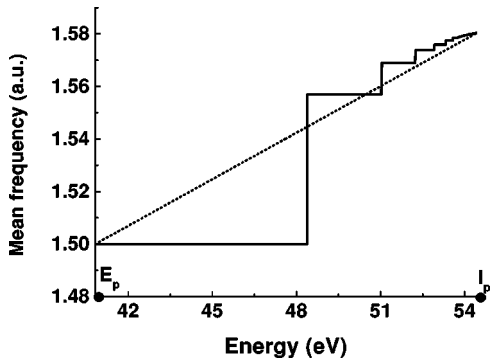

FIG. 7. Mean transition frequency $\bar{\Omega}$ in inelastic $e+He^+$ collisions between first excitation and ionization thresholds: solid curve. Approximation [Eq. (32)]: dotted curve.

narrow and $\bar{\Omega}(E)$ does not change much, its stepwise behavior can be replaced with a linear approximation

$$\bar{\Omega}(E \leqslant I_p) \approx \bar{\Omega}_0 + (\bar{\Omega}_I - \bar{\Omega}_0)\zeta(E), \tag{33}$$

where $\zeta(E)$ was introduced in Eq. (21). Above I_p, one has to match the known values of $\bar{\Omega}(E)$ at $E \gg I_p$ [45] and $E = I_p$. The relevant parameter is, once again, $G(E)=(E-I_p)/E_m$. Starting with $G(E)\approx 2$, the relative contributions of excitation and ionization channels quickly approach constant and $\bar{\Omega}(E)$ quickly reaches its asymptotic value $\bar{\Omega}_\infty$. We use the fit

$$\bar{\Omega}(E \geqslant I_p) \approx \bar{\Omega}_\infty - (\bar{\Omega}_\infty - \bar{\Omega}_I)\exp[-\mu G(E)]. \tag{34}$$

The constant μ is found by matching the threshold behavior of $\bar{\Omega}(E)$, yielding $\mu \approx 1$. Dependence on the exact value of μ is very weak.

III. RESULTS AND DISCUSSION

Figures 1 and 8 show the results of our calculations for He atom irradiated by 780-nm light. Since our model is based on tunneling, we do not show any calculations at $I < 2\times 10^{14}$ W/cm^2 ($\gamma > 1$) and at intensities above the barrier suppression intensity $I > 1.4\times 10^{15}$ W/cm^2.

In the calculations, we assumed constant laser intensity and propagated each trajectory for 200 fs. In principle, the probability of collisional ionization or excitation of a He^+ core can be significant during more than one approach of the active electron to the parent ion. In this case, the ionization probability is calcuated using the formula $P_{tot}=P_1+(1-P_1)P_2+\cdots$, where P_1 is the ionization probability during the most efficient collision, P_2 is the ionization probability during the second most efficient collision, and so on.

The results are virtually insensitive to how many collsions per each trajectory we include to calculate the probability of double ionization. Indeed, almost always there is only one ''hard'' collision (close encounter with the parent ion) per trajectory, after which the active electron does not return to the core.

It is important to emphasize that the results in Figs. 1 and 8 are insensitive to the specific model that relates the excitation and ionization cross sections to the impact parameter-dependent probabilities [see Eqs. (29)], with the exception of the nearly hard-sphere model [Eq. (30)]. For all three physically justified models, which exhibit correct large impact parameter behavior the results agree within a few percent. For the hard-sphere model the yield of He^{2+} shows no plateau at $I > 6\times 10^{14}$ W/cm^2 and is higher by up to a factor of 3 at $I > 10^{15}$ W/cm^2.

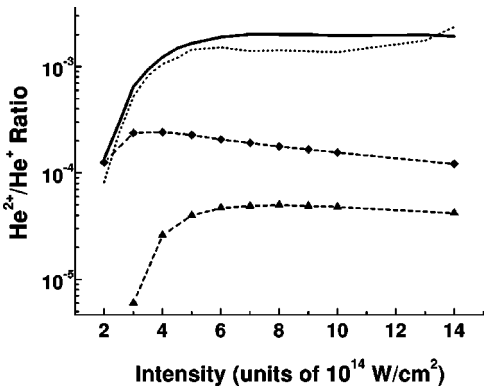

FIG. 8. Calculated ratio of doubly to singly charged He as a function of laser intensity. Complete recollision model, including all inealstic collision channels and the effects of the Coulomb potential: solid curve. Naive recollision model, that ignores both the Coulomb potential of the parent ion and collisional excitation: dashed triangles curve. Recollision model that ignores the Coulomb potential but includes both collisional ionization and collisional excitation: dashed-diamonds curve. Dotted curve shows sensitivity of the model to the ensemble of initial conditions for the active electron after tunneling: compared to the solid curve, this calculation only includes the radial velocity distribution.

A. Importance of collisional excitation and long-range core potential

The lowest curve (triangles) in Fig. 8 coresponds to the naive recollision model, which (i) ignores effects of the Coulomb potential and (ii) does not take into account collisional excitation. The calculated yield of He^{2+} relative to He^+ is almost two orders of magnitude below the experimental data of Ref. [1]. Taking into account the possibility of collisional excitation followed by laser-induced ionization (diamonds) brings the yield up by a factor of 3–40, depending on the laser intensity. Still, the results fall significantly below the experimental data. Furthermore, as long as the Coulomb potential of the ionic core is neglected, the yield of He^{2+} remains almost the same when trajectories are propagated for one laser cycle or for many laser cycles. Indeed, without the Coulomb focusing effect [14], if the electron misses the parent ion during the first return, it will have an even larger impact parameter during subsequent returns.

Next, we include the Coulomb potential of the parent ion into the calculation. The result, shown in Fig. 8 with solid line, agrees well with the experimental data of Ref. [1], except for the lowest intensity region, where the tunneling model is clearly inapplicable.

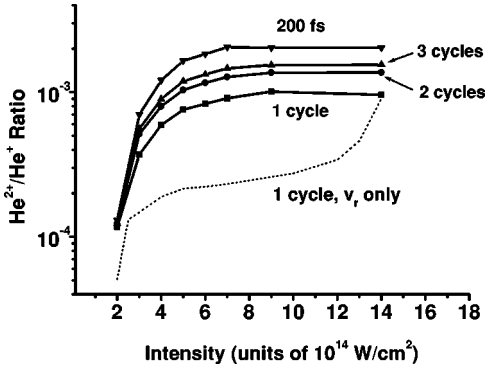

FIG. 9. The role of late returns in He double ionization. Top four curves correspond to terminating each active electron trajectory after 1, 2, and 3 cycles and after 200 fs. For the bottom curve only the radial velocity distribution of the active electron was included and each trajectory was terminated after 1 cycle.

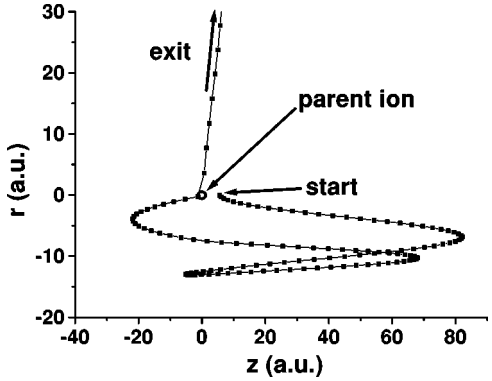

FIG. 10. Typical trajectory of the active electron, which demonstrates the effect of Coulomb focusing, from the moment of tunneling until departure from the interaction region after hard collision with parent ion.

To check the sensitivity of our results to initial conditions, we performed calculations with the ensemble that fixes $v_z=0$, $z=z_0$, and $r=0$ and only includes the distributon of transverse velocity v_r after tunneling (v_r is responsible for transverse spread of trajectories). Results shown in Fig. 8 with dashed line are close to the calculations with full ensemble of initial conditions.

Figure 8 clearly demonstrates that the Coulomb potential of the ionic core plays a crucial role in ensuring relatively high yield of He^{2+}. We now look at physical effects caused by the interaction of the active electron with the core potential after tunneling.

B. Coulomb focusing and the role of late returns

Figure 9 shows the relative yield of He^{2+} when each active electron trajectory is propagated for progressively larger number of laser cycles after tunneling. In the calculation for, say, three laser cycles, we propagated every trajectory for three cycles after tunneling, irrespective of the laser phase at birth. The lowest curve, labeled ''1 cycle, v_r only'' shows results where all trajectories were started with zero initial velocity component along laser polarization, $v_z=0$, and propagated for one laser cycle.

It is clear from Fig. 9 that late returns play an important role in double ionization. The typical trajectory that displays Coulomb focusing is shown in Fig. 10. The starting point and the direction in which the electron leaves after hard collision (a little over two cycles after start) are indicated with arrows. Note that the minimal distance to the parent ion during the first approach to the nucleus is very large for this trajectory (≈ 12.5 a.u.), corresponding to relatively large initial transverse velocity v_r. Statistically, there are more trajectories with relatively large initial transverse velocity v_r (which miss the core on the first return) than with negligible v_r (which experience hard collision during the first return).

Coulomb focusing is important already during the early evolution of trajectories (times shorter than one laser period), as stressed by comparing the curve labeled ''1 cycle'' with the curve labeled 1 cycle, v_r only (see Fig. 9). The difference stems from initial conditions: for the lower curve initial velocity along laser polarization is set to zero, $v_z=0$ (v_r is varied, of course). Physically, in the case of $v_z<0$ the electron starts towards the core and experiences soft scattering at the early stage of the trajectory. This reduces v_r and the spreading of trajectories. Consequently, a larger fraction of the trajectories experience hard collision with the parent ion during the first cycle, as is clear from comparing one-cycle results with and without v_z distribution. As seen in Fig. 9, the difference between the two curves disappears at high intensities; the strong field quickly accelerates the electron away from the core, overwhelming the inital longitudinal velocity component. We stress, however, that the long-term probability of double ionization is much less sensitive to the initial conditions, as is clear from comparing results in Fig. 8 (dashed and solid curves).

C. Energy gain in soft collisions and transient trapping in Rydberg states

In the naive recollision model, the energy of the electron at the moment of return is fixed by the laser phase at the instant of tunneling. In particular, the highest instantaneous energy at the moment of return, $3.2U_p$, corresponds to the phase of tunneling $\phi^*\approx 17°$. This is no longer the case when the Coulomb potential of the parent ion is taken into account.

First, many electrons have negative energy at the moment of return, meaning that they are transiently bound. Transient trapping occurs after tunneling; in the model electrons are placed outside the potential well, on the outer side of the tunneling barrier. One of the characteristic long-living quasibound trajectories is shown in Fig. 11. After tunneling, soft scattering off the parent ion sends the electron on a nearly circular Kepler trajectory, where the electron stays bound for nearly 100 fs until finally leaving for good.

Second, we found that multiple soft scattering nearly removes the sensitivity of the maximim electron energy at the moment of collision to the phase of the laser field at which the trajectory started. Qualitatively, every soft scattering gives a ''new start'' to the trajectory, with new initial phase and new initial velocity. Multiple scattering suppresses the sensitivity to the initial phase of birth, and while $3.2U_p$ remains the maximum energy, the electrons have the moment

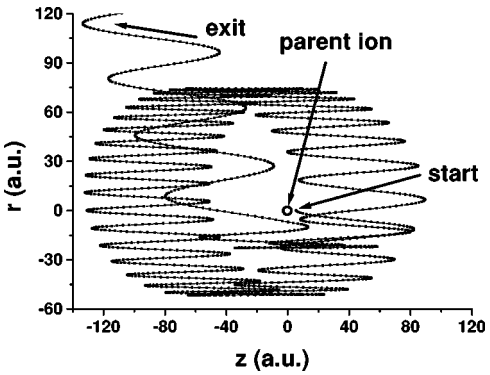

FIG. 11. Long-term trapping of an active electron into a Rydberg orbit after tunneling.

of return, these high-energy electrons appear for virtually any phase of birth. Consequently, we found that almost all initial phases contribute significantly to double ionization, provided the tunneling probability at these phases is nonnegligible.

IV. CONCLUSIONS

To study the physics of double ionization of atoms in intense laser fields, we had to address two problems important in other areas of physics.

(1) *Inelastic electron-ion collision in intense field.* We have demonstrated that in intense field-assisted collisions one can distinguish a nonadiabatic stage, which is preceeded and followed by adiabatic evolution. The nonadiabatic stage, which leads to excitation or ionization of the atom (ion), can be treated as field free in first approximation, provided the laser field is included during the adiabatic stages of collision and all collision channels are included. This result, derived using the theory of semisudden perturbations, supports the results of Refs. [44,46] for very high electron energies, where it was directly verified using Born approximation.

(2) *Total inelastic cross sections.* This problem is of great interest in physics of electron-atom (ion) collisions and in plasma physics. The semi-empirical scaling laws, which relate total excitation cross sections to total ionization cross sections, were traced to simple collision models based solely on energy and momentum conservation. Therefore, they should apply not only to He, but also to other atoms and ions, giving a simple prescription for estimating total excitation cross sections above the ionization threshold from experimentally measured ionization cross sections.

Based on the physical processes that play a key role in double ionization in our model, we can suggest several experiments to verify model predictions. Firstly, there is a clear effect in double ionization with few-cycle pulses: since late collisions between active electron and parent ion would no longer be possible, the relative efficiency of double ionization will be reduced. This effect, which is not limited to He and should be present for other noble gases, was recently observed for Ne in Ref. [47]. Second, importance of collisional excitation implies that a lot of excited singly charged ions should be observed in experiments with few-cycle pulses. Finally, one can control the efficieny of late returns by using laser pulses with time-dependent ellipticity [48], thereby suppressing double ionization.

ACKNOWLEDGMENTS

The authors have benefited from valuable and stimulating discussions with P. Corkum. We appreciate communications with A. Becker, W. Becker, L. DiMauro, F. Faisal, P. Knight, D. Lappas, and H. Muller. We are thankful to L. DiMauro for sending the experimental data of Ref. [1].

APPENDIX: THEORY OF SEMISUDDEN PERTURBATIONS

Considering the collision of an electron with an ion in the presence of a laser field, we encounter a rather typical situation for many physical problems. Namely, during the time of collision τ the effect of the laser field on the evolution of a quantum state of the ion was small, while the effect of the field-free part of the ionic Hamiltonian was as important as the electron-electron interaction. Here we are dealing with an example of a large class of problems, where the Hamiltonian of a system interacting with external perturbation (either weak or strong) can be partitioned into two parts, with one of them negligible during the perturbation. This class of problems can be efficiently analyzed using the theory of semisudden perturbations [49,50].

Let us consider a general quantum system with the Hamiltonian $\hat{H}$, interacting with an external perturbation $\hat{V}(t)$ that acts during a time interval τ near the moment t_c. We assume that the Hamiltonian $\hat{H}$ can be partitioned into $\hat{H}_0$ and $\hat{H}'$,

$$\hat{H}=\hat{H}_0+\hat{H}', \tag{A1}$$

where during the interaction τ the characteristic values of $\hat{H}_0(t_c)$, denoted as $\epsilon_0(t_c)$, are singnificantly different from $\epsilon'(t_c)$, the characteristic values of $\hat{H}'(t_c)$:

$$\epsilon'(t_c)\,\tau \ll \epsilon_0(t_c)\,\tau \sim 1. \tag{A2}$$

This inequality allows us to apply the general method of sudden perturbations [51] to find the time-evolution operator $\hat{S}(t,t')$ for the wave function $|\Psi_{\rm int}(t)\rangle$ in the interaction representation (the Dirac picture)

$$|\Psi_{\rm int}(t)\rangle=\exp\left(i\int^t dt'\,\hat{H}(t')\right)|\Psi(t)\rangle, \tag{A3}$$

where $|\Psi(t)\rangle$ is the wave function in coordinate representation (the Schrödinger picture). Let $\hat{S}_0(t,t')$ be the time-evolution operator for $|\Psi_{\rm int}(t)\rangle$ where $\hat{H}'$ has been neglected during the time interval τ near t_c. Note that $\hat{H}'$ cannot be neglected prior to t_c and must be included into $\hat{S}_0(t,t')$. For our specific problem of laser-assisted collisional excitation and/or ionization, $\hat{S}_0$ corresponds to field-free collision, promoting the electron from the ground state of He^+ to a superposition of excited states, but includes the effects of the laser field prior to collision.

We now develop a series in powers of ϵ'/ϵ_0, using the fact that $\epsilon'\tau \ll 1$

$$\hat{S}(t,t') = \hat{S}_0(t,t')\left[\hat{I} + \sum_{n=1}^{\infty} \hat{C}_n(t,t')\right], \tag{A4}$$

where $\hat{I}$ is the unity operator and $C_n = O[(\epsilon'/\epsilon_0)^n]$.

To find $\hat{S}_0(t,t')$ and $\hat{C}_n(t,t')$ we expand the interaction operator $\hat{W}(t)$ in the interaction picture,

$$\hat{W}(t) = \exp\left[i\int^t dt'\hat{H}(t')\right]\hat{V}(t)\exp\left[-i\int^t dt'\hat{H}(t')\right] \tag{A5}$$

in powers of (ϵ'/ϵ_0)

$$\hat{W}(t) = \sum_{n=0}^{\infty} \hat{W}_n(t), \tag{A6}$$

where $W_n = O[(\epsilon'/\epsilon_0)^n]$.

Before giving the specific expressions for the first terms $\hat{W}_n$ in this expansion, we note that for any expansion of the form [Eq. (A5)] the corresponding $\hat{S}_0(t,t')$ is found from the equation

$$i\frac{\partial \hat{S}_0(t,t')}{\partial t} = \hat{W}_0(t)\hat{S}_0(t,t') \tag{A7}$$

with the boundary condition $\hat{S}_0(t,t) = \hat{I}$, which is equivalent to the integral equation

$$\hat{S}_0(t,t') = \hat{I} - i\int_{t'}^{t} dt''\, \hat{W}_0(t'')\hat{S}_0(t'',t'). \tag{A8}$$

The first two terms in the expansion Eq. (A4) are [50]

$$\hat{C}_1(t,t') = -i\int_{t'}^{t} dt''\, \hat{S}_0^{-1}(t'',t')\hat{W}_1(t'')\hat{S}_0(t'',t') \tag{A9}$$

and

$$\hat{C}_2(t,t') = \frac{1}{2}\hat{C}_1^2(t,t') - i\int_{t'}^{t} dt''\, \hat{S}_0^{-1}(t'',t')\hat{W}_2(t'')\hat{S}_0(t'',t'). \tag{A10}$$

We now give the explicit expressions for $\hat{W}_0(t)$ and $\hat{W}_1(t)$. There are several mathematically equivalent forms of such expressions (see Ref. [50]), of which we will only give the most suitable for practical calculations:

$$\hat{W}_0(t) = \exp[i\hat{\alpha}(t)]\hat{V}(t)\exp[-i\hat{\alpha}(t)], \tag{A11}$$

$$\hat{W}_1(t) = [\hat{A}(t), \hat{W}_0(t)], \tag{A12}$$

where

$$\hat{\alpha}(t) = \int^t dt''\, \hat{H}_0(t'') + \int^{t_c} dt''\, \hat{H}'(t''), \tag{A13}$$

$$\hat{A}(t) = i(t-t_c)\int_0^1 d\mu\, \exp[i\mu\hat{\alpha}(t)]\hat{H}'(t)\exp[-i\mu\hat{\alpha}(t)]. \tag{A14}$$

It is often easier to use an alternative form for $\hat{W}_1$,

$$\hat{W}_1(t) = i(t-t_c)\int_0^1 d\nu\, \exp[i\nu\hat{\alpha}(t)][\hat{H}'(t), \hat{B}(\nu)] \times \exp[-i\nu\hat{\alpha}(t)] \tag{A15}$$

since the complexity of calculating the operator $\hat{B}(\nu)$ entering this formula,

$$\hat{B}(\nu) = \exp[i(1-\nu)\hat{\alpha}(t)]\hat{V}(t)\exp[-i(1-\nu)\hat{\alpha}(t)] \tag{A16}$$

is about the same as that for $\hat{W}_0(t)$.

[1] B. Walker, E. Mevel, Baorui Yang, P. Breger, J. P. Chambaret, A. Antonetti, L. F. DiMauro, and P. Agostini, Phys. Rev. A **48**, R894 (1993); B. Walker, B. Sheehy, L. F. DiMauro, P. Agostini, K. J. Schafer, and K. C. Kulander, Phys. Rev. Lett. **73**, 1227 (1994).

[2] *Multiphoton Processes*, ICOMP VIII, edited by L. F. DiMauro, R. R. Freeman, and K. C. Kulander (American Institute of Physics, Melville, NY, 2000).

[3] K. C. Kulander, K. J. Schafer, and J. Krause, in *Atoms in Intense Laser Fields*, edited by M. Gavrila (Academic, New York, 1992), p. 247; the most impressive experimental evidence is presented in M. J. Nandor, M. A. Walker, L. D. Van Woerkom, and H. G. Muller, Phys. Rev. A **60**, R1771 (1999).

[4] A. L'Huillier, L. A. Lompre, G. Mainfray, and C. Manus, J. Phys. B **16**, 1363 (1983); J. Phys. (France) **44**, 1247 (1983).

[5] D. N. Fittinghoff, P. R. Bolton, B. Chang, and K. C. Kulander, Phys. Rev. Lett. **69**, 2642 (1992); Phys. Rev. A **49**, 2174 (1994).

[6] A. Talebpour, S. Larochelle, and S. L. Chin, J. Phys. B **30**, L245 (1997); A. Talebpour, C.-Y. Chien, Y. Liang, S. Larochelle, and S. L. Chin, *ibid.* **30**, 1721 (1997); S. Larochelle, A. Talebpour, and S. L. Chin, *ibid.* **31**, 1201 (1998).

[7] K. Kondo, A. Sagisaka, T. Tamida, Y. Nabekawa, and S. Watanabe, Phys. Rev. A **48**, R2531 (1993).

[8] J. Parker, K. T. Taylor, Ch. W. Clark, and S. Blodgett-Ford, J. Phys. B **29**, L33 (1996); J. S. Parker, E. S. Smyth, and K. T. Taylor, *ibid.* **31**, L571 (1998); D. D. Dundas, K. T. Taylor, J. S. Parker, and E. S. Smyth, *ibid.* **32**, L231 (1999); J. S. Parker, D. H. Glass, L. R. Moore, E. S. Smyth, K. T. Taylor, and P. G. Burke, *ibid.* **33**, L239 (2000); J. S. Parker, L. R. Moore, E. S. Smyth, and K. T. Taylor, *ibid.* **33**, 1057 (2000).

[9] P. B. Corkum, Phys. Rev. Lett. **71**, 1994 (1993).

[10] K. J. Schafer, B. Yang, L. F. MiMauro, and K. C. Kulander, Phys. Rev. Lett. **70**, 1599 (1993).

[11] W. Becker, A. Lohr, and M. Kleber, Quantum Semiclass. Opt. B **7**, 423 (1995).

[12] See, e.g., B. Sheehy, R. Lafon, M. Widmer, B. Walker, L. F. DiMauro, P. A. Agostini, and K. C. Kulander, Phys. Rev. A **58**, 3942 (1998).

[13] M. Protopapas, C. H. Keitel, and P. L. Knight, Rep. Prog. Phys. **60**, 389 (1997).

[14] T. Brabec, M. Yu. Ivanov, and P. B. Corkum, Phys. Rev. A **54**, R2551 (1996).

[15] H. W. van der Hart and K. Burnett, Phys. Rev. A **62**, 013407 (2000).

[16] R. Grobe and J. H. Eberly, Phys. Rev. A **48**, 4664 (1993); D. G. Lappas, A. Sanpera, J. B. Watson, K. Burnett, P. L. Knight, R. Grobe, and J. H. Eberly, J. Phys. B **29**, L619 (1996); D. G. Lappas and R. van Leeuwen, *ibid.* **31**, L249 (1998); W.-C. Liu, J. H. Eberly, S. L. Haan, and R. Grobe, Phys. Rev. Lett. **83**, 520 (1999); C. Szymanowski, R. Panfili, W.-C. Liu, S. L. Haan, and J. H. Eberly, Phys. Rev. A **61**, 055401 (2000).

[17] M. Lein, E. K. U. Gross, and V. Engel, J. Phys. B **33**, 433 (2000).

[18] A. Becker and F. H. M. Faisal, J. Phys. B **29**, L197 (1996); **32**, L335 (1999); Phys. Rev. A **59**, R1742 (1999); Phys. Rev. Lett. **84**, 3546 (2000); F. H. M. Faisal, A. Becker, and J. Muth-Böhm, Laser Phys. **9**, 115 (1999).

[19] W. Becker, A. Lohr, and M. Kleber, J. Phys. B **27**, L325 (1994); G. G. Paulus, W. Becker, W. Nicklich, and H. Walther, *ibid.* **27**, L703 (1994); A. Lohr, M. Kleber, R. Kopold, and W. Becker, Phys. Rev. A **55**, R4003 (1997); R. Kopold and W. Becker, J. Phys. B **32**, 419 (1999); R. Kopold, D. B. Milosevic, and W. Becker, Phys. Rev. Lett. **84**, 3831 (2000).

[20] S. P. Goreslavskii and S. V. Popruzhenko, Phys. Lett. A **249**, 477 (1998); J. Phys. B **32**, L533 (1999); Éksp. Teor. Fiz. **117**, 895 (2000) [J. Exp. Theor. Phys. **90**, 778 (2000)]; S. P. Goreslavskii and S. V. Popruzhenko, Laser Phys. **7**, 700 (1997); **8**, 1013 (1998); **10**, 700 (2000).

[21] J. B. Watson, A. Sanpera, D. Lappas, P. L. Knight, and K. Burnett, Phys. Rev. Lett. **78**, 1884 (1997); see also A. Sanpera, J. B. Watson, S. E. J. Shaw, P. L. Knight, K. Burnett, and M. Lewenstein, J. Phys. B **31**, L841 (1998).

[22] R. Moshammer, B. Feuerstein, W. Schmitt, A. Dorn, C. D. Schroater, J. Ulrich, H. Rottke, C. Tramp, M. Wittmann, G. Korn, K. Hoffmann, and W. Sandner, Phys. Rev. Lett. **84**, 447 (2000).

[23] Th. Weber, M. Weckenbrock, A. Staudte, L. Spielberger, O. Jagutzki, V. Mergel, F. Afaneh, J. Urbasch, M. Vollmer, H. Giessen, and R. Dörner, Phys. Rev. Lett. **84**, 443 (2000); J. Phys. B **33**, L127 (2000).

[24] See, for example, P. Dietrich, N. H. Burnett, M. Yu. Ivanov, and P. B. Corkum, Phys. Rev. A **50**, R3585 (1994); J. B. Watson, K. Burnett, and P. L. Knight, J. Phys. B **33**, L103 (2000).

[25] M. Lewenstein, Ph. Balcou, M. Yu. Ivanov, A. L'Huillier, and P. B. Corkum, Phys. Rev. A **49**, 2117 (1994).

[26] R. Kopold, W. Becker, H. Rottke, and W. Sandner, Phys. Rev. Lett. **85**, 3781 (2000).

[27] S. V. Popruzhenko and S. P. Goreslavskii, J. Phys. B (to be published).

[28] A. M. Dykhne, Zh. Éksp. Teor. Fiz. **38**, 570 (1960) [Sov. Phys. JETP **11**, 411 (1960)]; *ibid.* **41**, 1324 (1961) [*ibid.* **14**, 941 (1962)].

[29] L. V. Keldysh, Zh. Éksp. Teor. Fiz. **47**, 1945 (1964) [Sov. Phys. JETP **20**, 1307 (1965)].

[30] A. M. Perelomov, V. S. Popov, and M. V. Terent'ev, Zh. Éksp. Teor. Fiz. **50**, 1393 (1966) [Sov. Phys. JETP **23**, 924 (1966)]; *ibid.* **51**, 309 (1966) [*ibid.* **24**, 207 (1967)]; A. M. Perelomov and V. S. Popov, *ibid.* **52**, 514 (1967) [*ibid.* **25**, 336 (1967)]; V. S. Popov, V. P. Kuznetsov, and A. M. Perelomov, *ibid.* **53**, 331 (1967) [*ibid.* **26**, 222 (1967)].

[31] M. V. Ammosov, N. B. Delone, and V. P. Krainov, Zh. Éksp. Teor. Fiz. **91**, 2008 (1986) [Sov. Phys. JETP **64**, 1191 (1986)]; N. B. Delone and V. P. Krainov, J. Opt. Soc. Am. B **8**, 1207 (1991); N. B. Delone and V. P. Krainov, *Multiphoton Processes in Atoms* (Springer-Verlag, Berlin, 1994).

[32] A. V. Chaplik, Zh. Éksp. Teor. Fiz. **45**, 1518 (1963) [Sov. Phys. JETP **18**, 1046 (1964)]; *ibid.* **47**, 126 (1964) [*ibid.* **20**, 85 (1965)].

[33] K. T. Dolder, M. F. A. Harrison, and P. C. Thonemann, Proc. R. Soc. London, Ser. A **264**, 367 (1961); B. Peart, D. S. Walton, and K. T. Dolder, J. Phys. B **2**, 1347 (1969); P. Defrance, F. Brouillard, W. Claeys, and G. Van Wassenhove, *ibid.* **14**, 103 (1981); C. Achenbach, A. Muller, E. Salzborn, and R. Becker, *ibid.* **17**, 1405 (1984).

[34] *Electron Impact Ionization*, edited by T. D. Märk and G. H. Dunn (Springer-Verlag, New York, 1985).

[35] H. Bethe, Ann. Phys. (Leipzig) **5**, 325 (1930).

[36] J. J. Thomson, Philos. Mag. **23**, 449 (1912).

[37] M. Gryzinski, Phys. Rev. **138**, A305 (1965); **138**, A322 (1965); **138**, A336 (1965).

[38] D. F. Dance, M. F. A. Harrison, and A. C. H. Smith, Proc. R. Soc. London, Ser. A **290**, 74 (1966); K. T. Dolder and B. Peart, J. Phys. B **6**, 2415 (1973); Rep. Prog. Phys. **39**, 693 (1976).

[39] A. I. Dashchenko, I. P. Zapesochnyi, A. I. Imre, V. S. Bukstich, F. F. Danch, V. A. Kel'man, Zh. Éksp. Teor. Fiz. **67**, 503 (1974) [Sov. Phys. JETP **40**, 249 (1975)].

[40] A. K. Das and N. C. Sil, J. Phys. B **17**, 3987 (1984); **17**, 4001 (1984).

[41] W.-J. Qian, Y.-B. Duan, R.-L. Wang, and H. Narumi, J. Phys. B **24**, L443 (1991).

[42] I. I. Sobelman, L. A. Vainshtein, and E. A. Yukov, *Excitation of Atoms and Broadening of Spectral Lines* (Springer-Verlag, Heidelberg, 1981).

[43] *Handbook of Mathematical Functions*, edited by M. Abramowitz and I. A. Stegun (National Bureau of Standards, Washington, DC, 1965).

[44] G. L. Yudin, Zh. Éksp. Teor. Fiz. **83**, 908 (1982) [Sov. Phys. JETP **56**, 511 (1982)].

[45] G. L. Yudin, Zh. Tekh. Fiz. **55**, 9 (1985) [Sov. Phys. Tech. Phys. **30**, 4 (1985)]; Zh. Tekh. Fiz. **57**, 1714 (1987) [Sov. Phys. Tech. Phys. **32**, 1024 (1987)].

[46] M. V. Fedorov and G. L. Yudin, Zh. Éksp. Teor. Fiz. **81**, 2013 (1981) [Sov. Phys. JETP **54**, 1061 (1981)].

[47] V. R. Bhardwaj, S. A. Aseyev, M. Mehendale, G. L. Yudin, D. M. Villeneuve, D. M. Rayner, M. Yu. Ivanov, and P. B. Cor-

kum, Phys. Rev. Lett. (to be published).
[48] M. Ivanov, P. B. Corkum, T. Zuo, and A. Bandrauk, Phys. Rev. Lett. **74**, 2933 (1995).
[49] G. L. Yudin, Zh. Éksp. Teor. Fiz. **80**, 1026 (1981) [Sov. Phys. JETP **53**, 523 (1981)].
[50] A. M. Dykhne and G. L. Yudin, *Sudden Perturbations and Quantum Evolution* (Uspekhi Fiz. Nauk Publishing House, Moscow, 1996) (in Russian).
[51] A. M. Dykhne and G. L. Yudin, Usp. Fiz. Nauk [Sov. Phys. Usp. **20**, 80 (1977)]; Usp. Fiz. Nauk **121**, 157 (1977) [Sov. Phys. Usp. **21**, 549 (1978)].